Curricular Unit of Biomechanics of Motion
2019/20, Instituto Superior Técnico, Lisboa, Portugal

KINEMATIC ANALYSIS OF HUMAN MOVEMENT: GAIT AND STANDING LONG JUMP

André Vieira (83812)[1], Jeanne Evrard (95177)[2], Manuel Madeira (83836)[3] and Maria Parreira (83844)[4]

[1]*Instituto Superior Técnico,*
Integrated Master's in Biomedical Engineering
andre.s.vieira@tecnico.ulisboa.pt

[2] *Université Catholique de Louvain,*
Integrated Master's in Mechanical Engineering
jeanne.evrard@student.uclouvain.be

[3]*Instituto Superior Técnico,*
Integrated Master's in Biomedical Engineering
manuel.madeira@tecnico.ulisboa.pt

[4] *Instituto Superior Técnico,*
Integrated Master's in Biomedical Engineering
maria.parreira@tecnico.ulisboa.pt

ABSTRACT - *Kinematic analysis of motion is extremely relevant in the context of medicine and biology, sports performance and for the identification of injuries. In the present work, a kinematic analysis was performed to study the gait cycle and a standing long jump in a multibody biomechanical system. The data was acquired in the Biomechanics of Motion Lab at Instituto Superior Técnico and the 2D Multibody Model was defined with MATLAB. For the gait cycle, the movement of the knee and hip, as well as the velocity of the trunk throughout time was analyzed. The results were consistent with the literature, while some discrepancies were found in cadence and stride length, possibly attributed to the subject being focused on placing the feet in certain targets, causing the gait to be slightly slower than normal. For the standing long jump we analyse the take-off angle, height, distance and speed, the landing height and distance and flight and jump distances. The results were consistent with the literature, however the performance was not optimal, with the take-off angle being round 40°, far from the optimum 19-27°. This is normal considering the lack of technique for this specific motion of the subject under study. Overall, this mathematical model proved to be an important tool to tackle the problem at hands, with consistent results and allowing for a reliable analysis of motion.*

1 Introduction

Kinematics consists in the study of motion's acceleration, velocity and position, regardless of the forces involved during the performance of a movement. More specifically, multibody kinematic analysis consists of the evaluation of these components for each individual body in a system, by formulating and solving the equations of motion for each body part, thus being a great tool to assess performance and functionality of a given system. This has great use in different fields such as robotics or, in this case, biomechanics, by providing a non-invasive mean of collecting objective information and studying the motion of the body, limbs, and joints that occurs during movement.[1] For this reason, kinematic analysis is a huge contributor in many areas of expertise, from clinical rehabilitation to sports performance.

In the present work, two different motions were performed for analysis; the gait cycle, which is extensively described in literature, and a standing long jump.

1.1 Motion description: Gait

The gait movement consists of a repetitive pattern of steps and strides, with each cycle being measured from the instant one foot strikes the ground to the subsequent foot strike of the same foot. Each step corresponds to all the events between the heel strike of one leg and the heel strike of the opposite leg, with the stride corresponds to the whole gait cycle. The gait cycle consists in two main phases, the **stance phase** - the weight bearing part of the movement - and the **swing phase**, which, as the name suggests, corresponds to the swinging part of the movement, when the foot is non-weight bearing.

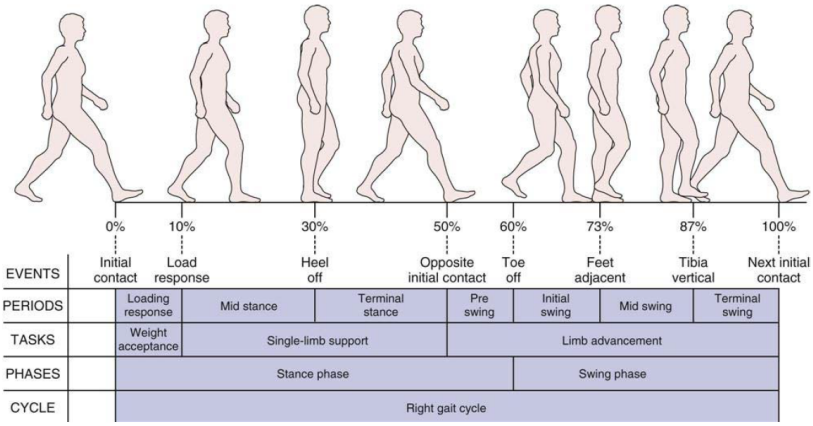

Figure 1.1: Gait cycle.[2]

This movement is illustrated in Figure 1.1; the stance phase begins when there is an initial contact of the heel with the ground (heel strike), marking the beginning of the loading response of the gait cycle, which then ends at the moment the opposite foot leaves the ground. From this moment to the moment where the center of mass is directly above the reference foot it is called the midstance. Finally, we reach the terminal stance, which ends at the moment of the opposite leg heel strike. The stance phase then ends with the pre-swing, marking the moment that the toes leave the ground, and giving rise to the swing phase. This phase corresponds to only 40% of the gait cycle,

and can be divided into two extra phases. The acceleration phase, from toe-off to midswing, and the deceleration, from midswing to heel strike.

Gait analysis is of great use specially in the clinical environment, since the kinematic and kinetic data obtained can be used to evaluate quantitatively the degree to which a patient's gait has been affected due to a certain disorder, such as cerebral palsy or neuromuscular disorders, by evaluating the deviations to the normal pattern of the gait.[3]

1.2 Motion description: Standing Long Jump

The standing long jump is a multi-joint movement that involves taking off and landing with both feet in order to achieve maximum horizontal distance It consists of a rather easy to perform movement, with the subject starting in a standing position, with both feet aligned and slightly apart, and then flexing both knees and the hip to gain the necessary balance. Finally, the subjects extends both knees and hip, while boosting thyself forward using only leg power, landing again with both feet. During this movement, the arms are also used for extra balance, being hyperextended before takeoff and immediately before landing, and flexed during the jump. At the moment of landing, there is again flexion of the hip, knees and arms to maintain the equilibrium.

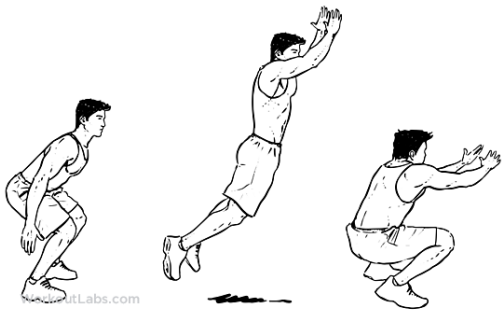

Figure 1.2: Standing long jump. Retrieved from *Standing Long Jump*. Accessed on 30/11/2019.

Standing long jump was an Olympic discipline until the year of 1938 but it is still considered a fundamental motor skill for a variety of sports where high velocity contractions are demanded.[4,5] As far as its application is concerned, it's a standard test for the assessment of lower limb explosive strength (a pivotal requirement in demonstrations of the maximum muscle force achieved in small periods of time[6]) and used to evaluate the levels of individual motor capabilities, as well as an objective metric for the teaching/training process with direct impact in education, sport and recreation.[7,8,9,10] Nevertheless, the performance on this movement is also highly influenced by the motor coordination and technical performance, rather than the explosive strength of the individual.[11]

2 Methodology

2.1 Data acquisition

The data acquisition step consists in measuring values from the physical world with sensors and then to transform them into digital data. Once received on the computer data can be treated, analysed, and used to build kinematic and dynamic models. More information on the data acquisition conditions can be found in Appendix A. The subject whose data was acquired was a 21 year-old woman, weighting 53kg and of height 1.67m.

To run our computational implementation of the next sections, please follow the instructions in the README.txt file (attached to the folder of the report).

2.2 Pre-Processing

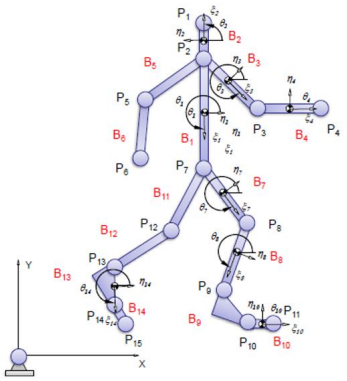

Figure 2.1: Model with 14 bodies (from B_1 to B_{14})and 15 points representing markers(from P_1 to P_{15})

Once the raw data is obtained, preprocessing is called for. Figure 2.2 references the functions implemented in Matlab for the preprocessing part. The projection of the 3D raw data to a 2D sagittal plane is performed - excluding the data from the y coordinate and considering only coordinates x,z. Upon projection, bodies with two markers need to be dealt with, namely hips and shoulder. The idea is to simply compute the midpoints, generating point P_2 for the shoulders and P_7 for the hips (Figure 2.1). The left and right heel points are not considered; thus, we go from 19 initial points to 15. Each body is characterized by two points (Figure 2.1), so 14 bodies can be identified in our model.

The function *ComputeAverageLength()* is used to deal with small inconsistencies in lenght of bodies due to the projection step. The file *static.xlsx* provides static data (2 seconds) used for reference. At each time step and for each body, the length is calculated between the two edge points of the body and the average is computed.

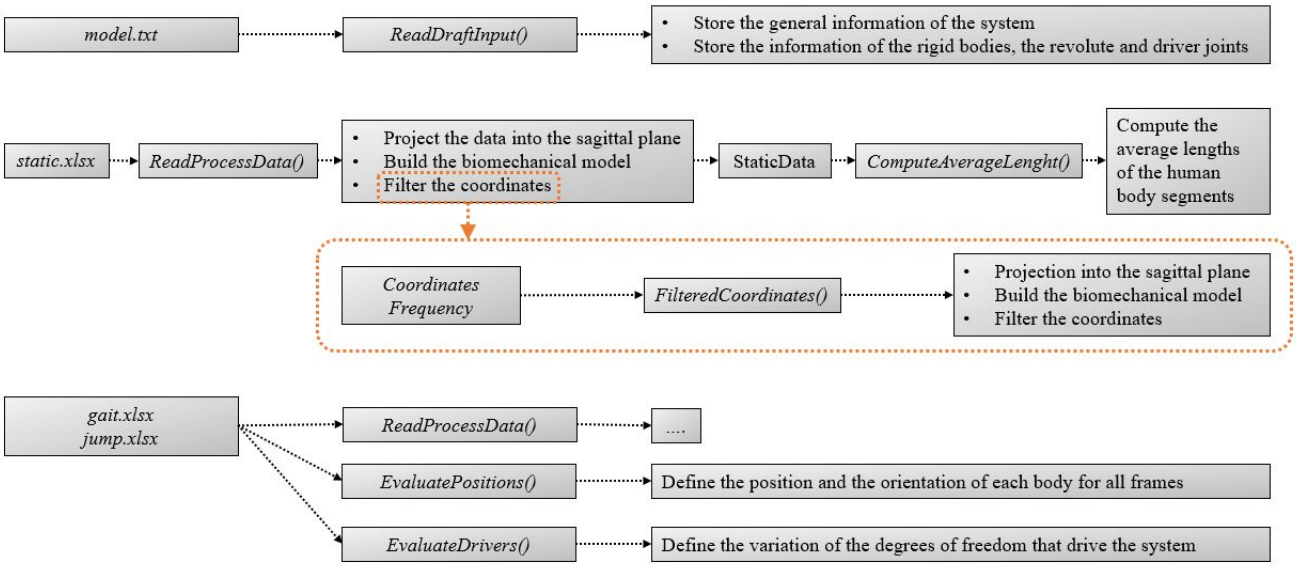

Figure 2.2: Map of the Matlab functions implemented for the pre-processing

The pre-processing steps described above have been extensively explained in class, so we won't get into too much deal. The filtering of the raw data, a step of the upmost importance, is described briefly in Appendix B. For the present project, only drivers of type I and III are implemented (in

function *EvaluateDrivers()*); type I drivers describe the absolute coordinates of the multi-body system and refer to body 1 (trunk). Drivers of type III are defined as the difference of the orientation of two bodies, with angles defined with respect to the horizontal axis and measured counterclockwise.

$$\theta_{ij} = \theta_j - \theta_i \tag{2.1}$$

Finally, *WritesModelInput()* will compute a summary of the data and variables created. It updates the driver's temporal data,as well as data from bodies, joints and drivers into .txt files. The structure of the output file is displayed on Appendix C.

2.3 Processing

Because there are 14 rigid bodies and 3 coordinates per body (x, y and θ), it leads to a total of 42 coordinates. In this multi-body system, there are 13 revolute joints which are represented by kinematic constrains. As we count 2 constraints per revolute joint, it makes a total of 26 kinematic restrictions. The number of degree of freedom (dof) is equal to $n_{dof} = n_{coordinates} - n_{constraints} = 42 - 26 = 16$ and the constraints defined by the joints are:

$$\Phi^(rev, 2) = (r_i + As_i'^P) - r_j + As_j'^P) = 0 \tag{2.2}$$

where *i, j* are the adjacent bodies, *r* = $[xy]^T$ (position in fixed frame), $s_i'^P$ refers to position in local frame and A is the rotation matrix given by θ. The degrees of freedom are driven by two types of driving constraints (see Table 2.1):

Table 2.1: Types of driving constraints

	Function	Equation of the constrains
Type I (3 implemented)	Positions the whole system in space, thanks to three coordinates *x,y* and θ	$\Phi(t) = z_i - z_i(t) = 0$ $\Phi(t) = x_i - x_i(t) = 0$ $\Phi(t) = \theta_i - \theta_i(t) = 0$
Type III (13 implemented)	Describes the angle between two bodies linked by a revolute joint	$\Phi(t) = \theta_{ij} - \theta_{ij}(t) = 0$ with $\theta_{ij} = \theta_j - \theta_i$

To fulfill the kinematic constrains, the following equation has to be respected:

$$\Phi(q, t) = 0 \tag{2.3}$$

with q the vector of generalized coordinates and t the given time. The system is nonlinear that is why Newton-Raphson method[12] is used (described in detail in Appendix D).

As we are also interested by the velocity and acceleration analysis, we derive the position and the velocity constraint equations with respect to time:

$$\begin{cases} \Phi(q,t) = 0 \\ \dot{\Phi}(q,t) = 0 \\ \ddot{\Phi}(q,\dot{q},t) = 0 \end{cases} \quad with \quad \begin{cases} \dot{\Phi}(q,t) \equiv \Phi_q \dot{q} = \nu \\ \ddot{\Phi}(q,\dot{q},t) \equiv \Phi_q \ddot{q} = \gamma \end{cases} \tag{2.4}$$

In order to derive the position variables,the function *spline()*(from MATLAB) is used to make the data smoother. This function makes a cubic spline interpolation with the scattered values stored in a vector. This is implemented in function *ReadInput()*.

3 Results and Discussion

3.1 Gait Analysis

Figure 3.1 displays the gait cycle acquired in the lab, after processing with the steps described in the previous section.

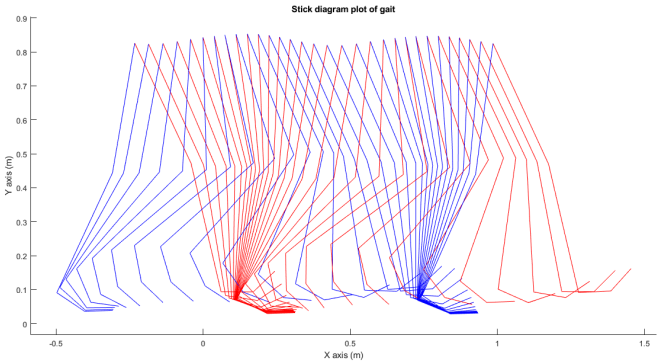

Figure 3.1: X and Z positions of the lower limbs during gait, plotted for a time step of 40ms. Red: left lower limb. Blue: right lower limb. Distances in meters.

The information displayed above, as well as the temporal information, can be used to calculate cadence, stride, and velocity of the gait:[13] cadence is given by steps/min and can be extrapolated if considering 2 steps in the total duration of the gait cycle (1.43s) - resulting in a cadence of 84 steps/min. On the other hand, stride, the total distance between two consecutive heel strikes by the same leg, in one complete gait cycle, can be derived from the positions of the toes and the value is of 1.24m . Finally, velocity can be inferred by calculating:

$$\text{velocity} = \frac{\text{stride} * \text{cadence}}{120} \ (m/s) \tag{3.1}$$

which gives a velocity of 0.87 m/s. However, this data is given for only one full cycle - in fact, for a total of 37 steps, the values differ - cadence is 109.1 steps/min, stride is 120.5 cm and velocity, as a consequence, is of 109.1 cm/s. This velocity is expected for women of age 20-29 (1.241 ± 0.071).[14] As for cadence, if recalculated for steps/sec we get a value of 1.81, which is below what is expected (2.08 ± 0.15).[14] Finally, for the stride length, the value obtained is actually close to the reference of 1.18 m;[14] the value of velocity is, however, consistent with the value of cadence obtained (lower than reference).

This data leads to the conclusion that this could be a slow walk rather than normal gait. However, it is of note that the subject was trying to step on the force sensor plates placed below her path thus possibly impairing the data collected, as the steps would have a bigger length and duration due to the effort of hitting certain targets on the ground. It should also be referenced that the results used for comparison are relative to only 15 subjects and there is great inter- and intra-subject variability described in literature.[13]

Finally, it's important to mention that the gait parameters calculated above, as well as other which may be as easily collected, are very useful tools for diagnosis of gait-related pathologies. In

this project, we assume the data refers to an healthy individual and don't explore pathological gait, as it is not the purpose of the project.

Displacements and velocities

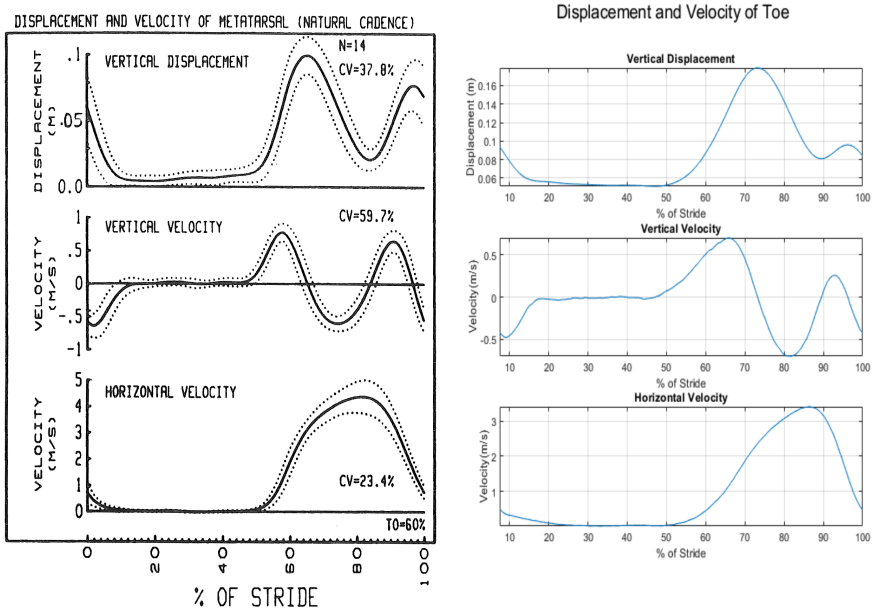

Figure 3.2: Vertical displacement (in meters), vertical velocity (in m/s) and horizontal velocity (in m/s) of the right metatarsal. Left: retrieved from *Winter(1987)*.[13] Right: obtained from lab data, after processing.

Figure 3.2 displays a side-by-side comparison of the results obtained from the lab data with those described in *Winter (1987)* for 14 subjects. The curves are indeed very similar except for the values of horizontal velocities - which are lower than expected -, consistent with the fact that this appears to be a slower-than-normal gait motion. It should be mentioned that the values plotted to the left are calculated from the center of mass of the body, rather than referring to a single marker placed in the metatarsal, which could be yet another source of small inconsistencies between data.

Joint Angle Displacement

Joint angles, being a relative measure of motion, do not allow us to draw conclusions about the absolute orientation of the bodies. However, because the trunk can be considered to be vertical during a walking motion (although not exact, this approximation simplifies interpretation), the hip angle is often used as to understand the orientation of the thigh in space, whereas the knee angle allows for the inference of the leg orientation in space; finally, the ankle relative angle will give a good estimate of the foot angle in space.

The relative angles were calculated as was described in the previous sections, with regards to the x-axis as 0° and increasing counter-clockwise. The differences are simply the subtraction of the θ of one of the segments adjacent to the joint by the θ of a second segment. However, for the purpose of side-by-side comparison, the angle displacement provided in Figure 3.3 is the result of

adding a constant to the joint angles of the knee and ankle, whose original values match the shape of the curve but not the exact values of the curve obtained in *Winter(1987)*.

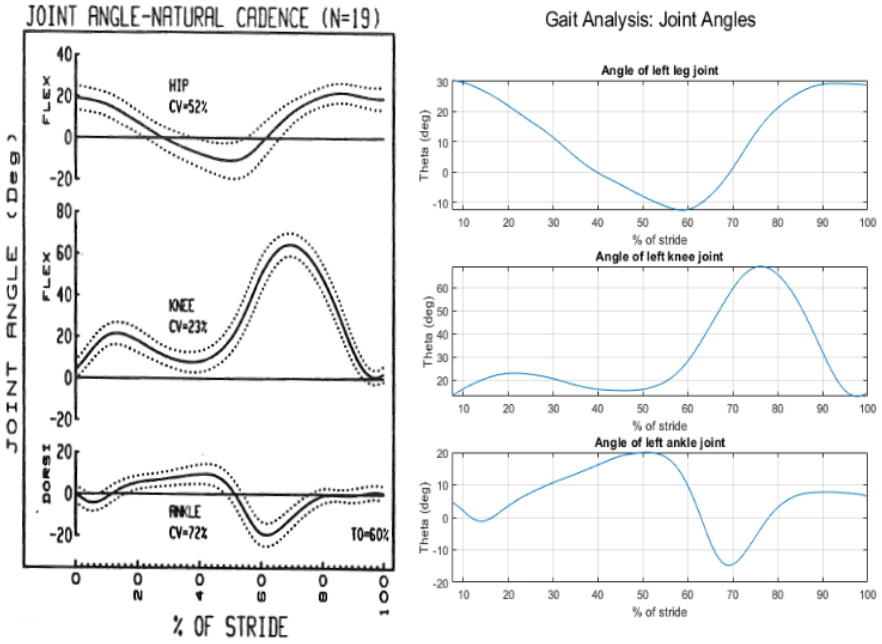

Figure 3.3: Joint angle (in degres) of hip (top), knee (center) and ankle (bottom. Left: retrieved from *Winter(1987)*.[13] Right: obtained from lab data, after processing.

For the curves above, note that positive angles are made to, in general, represent flexion of joints hip and knee (and dorsiflexion for the ankle), whereas negative angles represent extension (or plantar flexion). The curves are very similar, with the angles obtained falling within the deviations predicted. The exception is for the hip joint, whose angular amplitude is slightly bigger than expected (although it can be argued that results obtained through the lab data are merely a vertical shift of about 5 degrees) - again, this could be explained by the subject attempting to hit targets with their foot, thus not carrying a completely natural motion.

Upper body displacement, *e.g.* the motion of the arms during the walking cycle, was not studied for the gait motion, although it can be an important tool for detection of certain pathologies .

A final note is that any regular, repeated motion will have a pattern which is characteristic of each subject under study - inter-subject variability is the reason why large databases of biomechanical motion data are of the upmost importance to establish a transverse pattern - but one must also consider intra-subject variability inherent to our physical, as well as psychological status. With all of these variants, it is indeed impressive how the gait can be used, with extensive literature on the subject and precision on the results, as a form of diagnosis.

3.2 Standing Long Jump

For the analysis of the standing long jump (SLJ), the first step was to understand which components of the kinematic analysis were relevant to this type of motion. In fact, while for children the SLJ is determined only by the horizontal velocity at take-off moment, other factors have increasing preponderance through the growing process as a consequence of the improvement of motor

coordination. Thus, the proficiency of the standing long jump for adults depends mainly on three major components: horizontal velocity at take-off, take-off angle and arm swing during a jump.[15] Moreover, as far as adult females are concerned, it was shown that might not exist significant correlations between the SLJ performance and anthropometry: a greater muscle mass or longer leg can't explain by themselves the superior jumping performance.[16]

In order to have a more precise characterization of our SLJ kinematic analysis, we started by defining some interesting variables. Those variables are represented in Fig. E.1, present in Appendix E.

In the analysis, the center of mass (CoM) of the body was defined as the center of the rigid body corresponding to the trunk (body 1 in our kinematic model), although it is usually defined as slightly below this point. The jumper's take-off speed and take-off angle were calculated from the horizontal and vertical speed of the jumpers centre of mass at the instant of take-off, through the following expressions: $\nu = \sqrt{\dot{x}^2 + \dot{y}^2}$ and $\theta = \arctan \frac{\dot{x}}{\dot{y}}$, evaluated at the take-off instant. The take-off height and take-off distance were the vertical and horizontal distances of the jumper's centre of mass relative to the take-off line. Likewise, landing height and distance were the vertical and horizontal distances of the jumper's CoM relative to the location of the toes at the instant of landing. The flight distance was defined as the distance traveled by the center of mass between the two previously mentioned instants, while the jump distance was considered to be the sum of the three aforementioned distances. Values can be found in Table 3.1.

Table 3.1: Values obtained for the variables of interest of the SLJ, using the kinematic model computed for this motion.

h-takeoff (m)	**d-takeoff** (m)	θ**-takeoff** $(^\circ)$	ν**-takeoff** (m/s)	**d-flight** (m)	**h-landing** (m)	**d-landing** (m)	**d-jump** (m)
1.1882	0.3998	40.8131	1.7810	0.5950	0.9148	0.1298	1.1246

In order to give some meaning to the values above, they were compared with the results obtained for physically active males at maximum effort jumps, with these results being shown in Fig. E.2 in Appendix E.

For the specific take-off angle obtained, these results show that our take-off and landing heights are clearly above the expected - around 1m and 0.6 m, respectively (even though the difference between them is consistent with the usual differences). The landing distance is also below expectation ($\sim$0.2 m), while the take-off distance is also smaller ($\sim$0.5 m was expected). Regarding the take-off speed, it is also below expectations ($\sim$3.3 m/s). Finally, as far as the success metric of SLJ is concerned, the results obtained are clearly inferior from a successful performance point of view.

In order to enrich our analysis, we also compare the results obtained from the kinematic analysis with the expected main joint angles, positions and velocities throughout the SLJ. The results obtained and the expected ones are represented in Fig. 3.4 and Fig. 3.5.

Overall, it is possible to observe that the positions and velocities are concordant with the results usually described in the literature.

Given this, we may conclude that, from the technical point of view, the SLJ carried out is quite good. Nevertheless, there were some flaws observed from the performance point of view: even though our subject was an adult female and is being compared with physically active males, the differences were huge and can't be assigned only to this fact. The first relevant point is the take-off angle itself: the fact that it is near 40° can directly convey the message that the movement in our experiment was far from being optimal. In fact, for increasing take-off angles, the jumper spends a

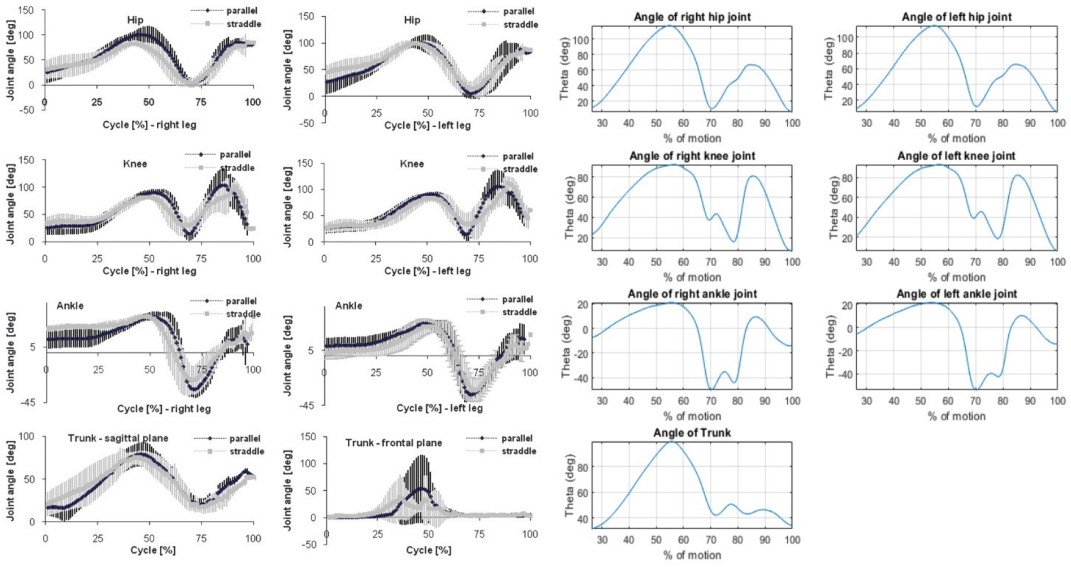

Figure 3.4: Main joint angles (ankle, knee, hip, pelvis, and trunk) during the SLJ. For the expected values, the ones to be considered in this case are the ones corresponding to parallel feet position. Retrieved from *Krzysztof et al.*[17]

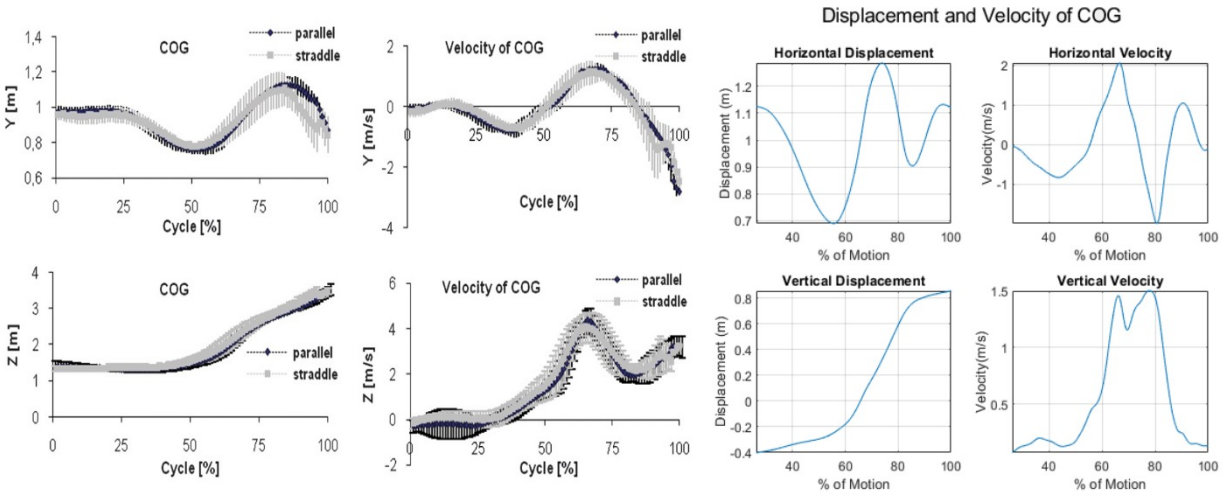

Figure 3.5: Trunk segment in the vertical, horizontal, and side positions and the value of the speed of center of mass through. For the expected values, the ones to be considered in this case are the ones corresponding to parallel feet position. Retrieved from *Krzysztof et al.*[17]

greater fraction of his muscular force overcoming body weight and, so, the take-off speed naturally decreases.

Usually, the range of the take-off angles in the best jumps with arm swinging is 29°- 37°.[18] In fact, for physically active males, it was observed that these angles also correspond to their preferred take-off angles, although the calculated optimum take-off angles is lower (19–27°).[19]

Actually, in the flight phase of the standing long jump, the centre of mass of the jumper behaves like a projectile in free flight. However, the optimum projection angle that maximises the distance of the jump is not expected to be 45° as the classical physical solution. A projection angle of 45° is only appropriate if the magnitude of the projection speed generated by the jumper is the

same for all projection angles. For example, it's known that in the long jump, javelin, and shot put the projection speed of the athlete (or implement) is known to decrease with increasing projection angle, *i.e.* the athlete has a bias towards the production of horizontal speed. In the SLJ, this bias still holds as well and, so, the take-off speed decreases with increasing take-off angle because the jumper must expend a greater fraction of the take-off force in overcoming their body weight.[19] This is the explanation for the fact that the take-off obtained of 40°is clearly not a good indicator. As it was shown, the take-off angle can be used to define all the other variables by Fig. E.2 and, so, all the performance will be affected by this value.

Besides, another cause for the small total jump distance observed may be assigned to the fact that the motion was not performed in a maximum effort assay. This was a consequence of the data acquisition constraints (one of the markers jumped off of the appropriate place whenever the maximum effort was performed) and will be analyzed along the dynamic component of this project, since it requires to know the values of the forces applied, through time. Nevertheless, the small take-off velocity obtained is a clear indicator of this fact. Given this, the analysis of the obtained EMG signals is also left for the second part of this project, since, intuitively, it may be more easily related with dynamic data than the mere kinematic analysis.

4 Conclusion

The musculoskeletal system's main goal is providing mobility and sustaining load through complex and highly coordinated mechanical interactions between bones, muscles, ligaments and joints so, understanding the kinematics of its motion has an important value in the context of medicine and biology, as well as for the study of mechanical factors that play a role in this system. Since each human being has the goal of moving efficiently, kinematic assessment reveals to be very useful, since it allows to obtain information about each body joint and segment and identify movement inefficiencies.

Regarding the results of our analysis, they revealed to be consistent with those described in literature and so this fact leads us to infer that our implementation of the kinematic analysis for both movements considered was successful. Any inconsistencies that cannot be attributed to the subject can be interpreted as a consequence of the computation methods used: truncation errors, filtration (which may not remove all the noise in data, thus being inefficient, or remove noise but also relevant signal), as well as the approximations performed for analysis (*e.g* consider the heel as the CoM of the foot).

For the gait motion, results are as expected but reveal that the motion could in fact be a slow gait rather than a natural gait. This analysis witnesses how the inter-subject variability needs to be considered when drawing conclusions from biomechanical data. Gait analysis results are not extensively exposed, since SLJ motion is more interesting from a pedagogical point-of-view.

As far as the standing long jump is concerned, it was possible to observe that the results obtained by our subject were clearly inferior to the ones described for maximum effort assays of physically active males. An interesting point in this analysis was that it was possible to establish relations between all the other variables of interest and the take-off angle and, so, as the take-off angle was far from the optimal range, this explains the performance observed. Nevertheless, the hypothesis that an extra factor for that performance is the non-maximal effort of our subject is also raised, although it can only be confirmed through a dynamic analysis for this data.

Bibliography

[1] "What is kinematic analysis?." https://vhc.missouri.edu/small-animal-hospital/motion-analysis-laboratory/what-is-kinematic-analysis/. Accessed: 2019-11-30.

[2] I. S. T. Integrated Masters in Biomedical Engineering, "Biomechanics of Human Motion 2019-2020 - week 04," 2019.

[3] P. Filipe and P. Pereira, "Gait Analysis in Patients Recovering from Total Joint Replacement Using Body Fixed Sensors," 2015.

[4] L. Szerdiová, D. Simšik, and Z. Dolná, "Assessment of kinematics of sportsmen performing standing long jump in 2 different dynamical conditions," vol. XIX, no. 1, pp. 85–94, 2012.

[5] K. R. M. Ackala and J. A. S. Todo, "Biomechanical Analysis of Standing Long Jump From Varying Starting Positions," pp. 2674–2684, 2013.

[6] R. U. Newton and W. J. Kraemer, "Developing explosive muscular power: Implications for a mixed methods training strategy," 1994.

[7] J. R. Fernandez-Santos, J. L. Gonzalez-Montesinos, J. R. Ruiz, D. Jiménez-Pavón, and J. Castro-Piñero, "Kinematic analysis of the standing long jump in children 6- to 12-years-old," *Measurement in Physical Education and Exercise Science*, vol. 22, no. 1, pp. 70–78, 2018.

[8] G.-G. . M. O. Popeska, B., "Structure of motor space in children at 7 year age," *Physical Education and Sport*, vol. 48, p. 19–24, 2009.

[9] R. Pišot and J. Planinšec, "Motor structure and basic movement competences in early child development," *Annales Kinesiologiae*, vol. 1, pp. 145–165, 12 2010.

[10] J. T. Viitasalo, "Evaluation of explosive strength for young and adult athletes," *Research Quarterly for Exercise and Sport*, vol. 59, no. 1, pp. 9–13, 1988.

[11] M. Lorger, M. Hraski, and Hraski, "The effects of motor learning on results of standing long jump performed bby female students," *Sport Science*, vol. 5, 06 2012.

[12] P. E. Nikravesh, *Computer-aided Analysis of Mechanical Systems*. Upper Saddle River, NJ, USA: Prentice-Hall, Inc., 1988.

[13] D. Winter, *The biomechanics and motor control of human gait*. University of Waterloo Press, 1987.

[14] R. B. Dale, "21 - clinical gait assessment," in *Physical Rehabilitation of the Injured Athlete (Fourth Edition)* (J. R. Andrews, G. L. Harrelson, and K. E. Wilk, eds.), pp. 464 – 479, Philadelphia: W.B. Saunders, fourth edition ed., 2012.

[15] M. Hraski, Hraski, and I. Prskalo, "Comparison of standing long jump technique performed by subjects from different age groups," *Baltic Journal of Sport and Health Sciences*, vol. 3, pp. 2–12, 09 2015.

[16] W.-L. Wu, J.-H. Wu, H.-T. Lin, and G.-J. Wang, "Biomechanical analysis of the standing long jump," *Biomedical Engineering: Applications, Basis and Communications*, vol. 15, pp. 186–192, 2003.

[17] M. Krzysztof, J. Stodółka, A. Siemieński, and M. Čoh, "Biomechanical analysis of standing long jump from varying starting positions," *Journal of strength and conditioning research / National Strength Conditioning Association*, vol. 27, 05 2012.

[18] L. Szerdiová, D. Simsik, and Z. Dolná, "Assessment of kinematics of sportsmen performing standing long jump in 2 different dynamical conditions," *Metrology and Measurement Systems*, vol. 19, 01 2012.

[19] M. Wakai and N. Linthorne, "Optimum take-off angle in the standing long jump," *Human movement science*, vol. 24, pp. 81–96, 03 2005.

[20] I. S. T. Integrated Masters in Biomedical Engineering, "Biomechanics of motion laboratory guide," 1°semester 2019/20.

[21] D. A. WINTER, "Biomechanics and motor control of human movement," p. 70, 2009.

Appendix A

Data acquisition

During the laboratory session organised at University, one volunteer had to execute first the gait cycle and then the movements predefined by each group. On the body of the subject, 19 markers were placed on relevant anatomic points as shown on Figure A.1. These passive markers reflect the incoming infrared radiation (IR) so that the cameras can track the position of each points. A motion capture system composed of 14 cameras is installed in the laboratory to this end.

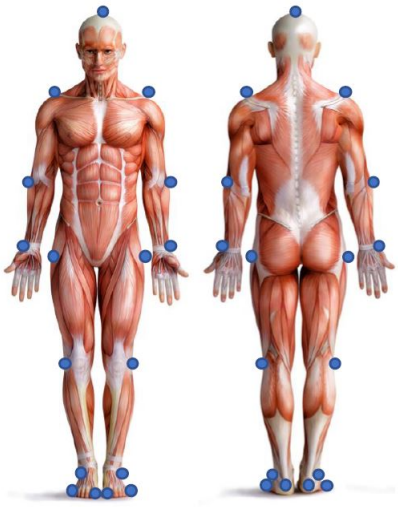

Figure A.1:
Position of the 19 retroreflective markers[20]

4 electromyography (EMG) electrodes were placed on muscles of the leg: the Gastrocnemius Medialis, Tibialis Anterior, Rectus Femoris and Biceps Femoris. They were used to collect the muscle activities from these 4 muscles. The subject had to walk along 3 force plates laid down on the floor. The 3 components of the ground reaction force and the trajectory of the center of pressure were calculated thanks to these platforms. In the first part of the project the data collected by the EMG and the platforms will not be analysed but it will be of use for the dynamic analysis.

Appendix B

Filtering

The function *FilteredCoordinates()* is based on the method that uses the residual analysis,described by *Winter(2009)*.[21] This method is a good compromise between reducing the noise present in the raw data while keeping the useful information. To determine which cut-off frequency f_c is the best, we process a residual analysis of the difference between filtered $\hat{X}_i$ and unfiltered X_i signals. This is computed over a wide range of cut-off frequencies (in the present case, 0.1Hz to 10Hz with a step of 0.1 Hz). For a gait cycle, the cut-off frequencies normally range between 2 and 6 Hz.[21]

The residual R is expressed as follows, where N is the number of samples in the signal:[21]

$$R(f_c) = \sqrt{\frac{1}{N}\sum_{i=1}^{N}(X_i - \hat{X}_i)^2} \qquad \text{(B.1)}$$

InFigure B.1, it can be observed the difference between the filtered and non filtered data. Indeed, the final curve is smoother thanks to the noise cancellation.

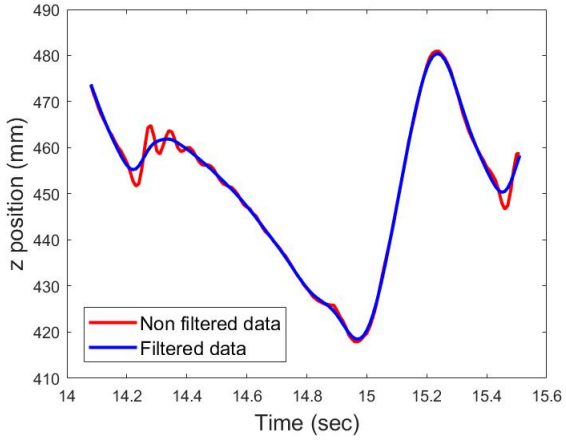

Figure B.1: Gait cycle:
z coordinate of the right knee over time.

The stopping criteria used, as a way to obtain f_c, was the correlation for the linear regression R^2 - valued at 0.92; initially, the value of 0.95 was initially used but after noting that it caused oscillations in the velocity and acceleration splines of the drivers it was considered too strict and the constraint was relaxed to first value mentioned.

Appendix C

Structure of the biomechanical models

Function*WritesModelInput.m* will generate 17 files: one with the structure observed in Figure C.1, named "BiomechanicalModel_(motion name, either gait or jump).txt", and one file for each one of the drivers defined for the motion under analysis, named "(motion name)(number of driver, 1 to 16).txt".

Store the general information

	NBody	NRevolute	NGround	NDriver
1				

Store the rigid body information

	Body number	X_i	Y_i	θ_i	Center of mass i	Length i
1 ↓ 14						

Store the revolute joint information

	Rev. joint number	Body i	Body j	ξ_i	η_i	ξ_j	η_j
1 ↓ 13							

Store the driver information: driver of type I or III : Do not concern the type of joint

	Driver number	Driver type	Body i	Coordoninate number	Body j	Coordoninate number	File name
1	..	I	i	1, 2 or 3			.txt
↓ 16	..	III	i		j		.txt

Store the time information

	t_{start}	t_{step}	t_{end}
1			

Figure C.1: Structure of files "BiomechanicalModel_gait.txt" or "BiomechanicalModel_jump.txt", clarifying to which variables the values refer to.

Appendix D

Newton-Raphson Method[12]

In this method, the convergence is quadratic, meaning that the square of the error at one iteration is proportional to the error at the next iteration. This method can be described by the following steps:

1. Define an initial estimate for solution: $q_{i=0} = q^0$
2. Start iterative process: $q_{i+1} = q_i + |\Delta q_i|$
3. if the magnitude of the larger residual of vector $|\Delta q_i|$:
    - is larger than a predefined threshol ϵ, i.e. $|\Delta q_i(j)| > \epsilon$ for any $j = 1, ..., \mathrm{n_{coord}}$, the iteration process continues;
    - is smaller than a predefined threshol ϵ, i.e. $|\Delta q_i(j)| < \epsilon$ for any $j = 1, ..., \mathrm{n_{coord}}$, the iteration process is stopped.

A value of 10^{-6} is used for ϵ and additionally a maximal number of iterations is defined (12); however, it could be observed that after 3 iterations, in general, the solution is found. The Newton-Raphson method can be expressed as follows:

$$\begin{cases} q_{i+1} = q_i - [\Phi_{q_i}(q_i, t)]^{-1}\Phi(q_i, t) & \text{(D.1)} \\ |q_i - q_{i+1}| \leq \epsilon & \text{(D.2)} \end{cases}$$

where the jacobian matrix of the position constraints is notated as Φ_{qi}. For the first step, we need initial values for our data. The function *Body2q()* is implemented in this purpose. It sets up the initial conditions to launch the Newton-Raphson method.

Appendix E

Standing Long Jump

Below is an illustration of the variables used for analysis, as well as a description of their calculation methods.

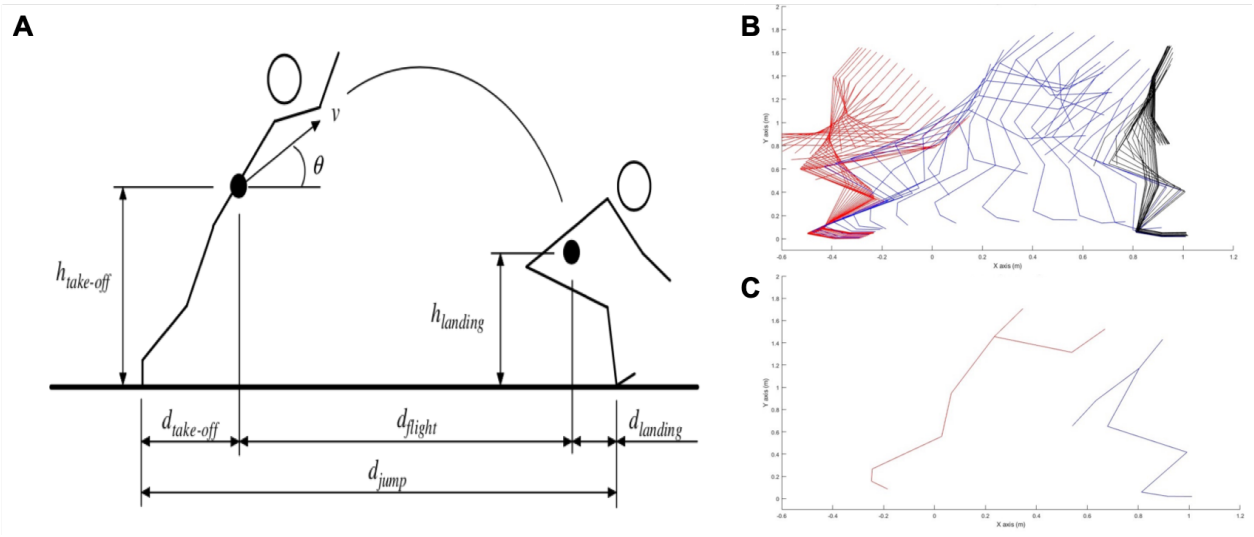

Figure E.1: Variables of interest for the kinematic analysis of the standing long jump. A: representation of the variables of interest. θ and ν correspond to take-off angle and take-off speed, respectively. Retrieved from *Wakai et al.*[19] B: representation of the biomechanical model through time obtained as a result of the kinematic analysis for the standing long jump - not all the frames are represented. C: Frames chosen as the taking-off instant (frame 210) and the landing one(frame 255). The former was defined as the first clear frame in which the jumpers feet were observed to break contact with the ground, whereas the latter was defined as the first clear frame in which the jumpers feet were observed to contact the landing pit.

Furthermore, the fitted data of a Standing Long Jump study used for comparison[19] can be seen in Figure E.2. The values obtained from our analysis were compared to this data, although not represented on the original plots. Conclusions of this analysis can be found in the Results section.

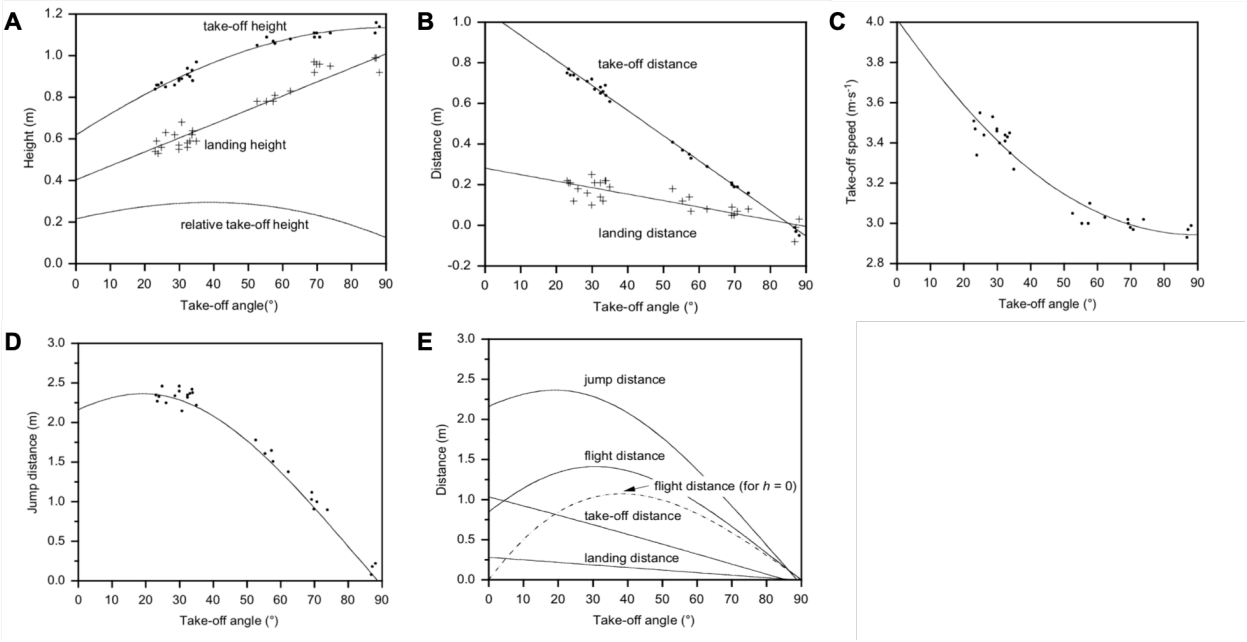

Figure E.2: Fitted data for physically active at maximum effort jumps for different take-off angles. A: Take-off height and landing height as a function of the take-off angle. The relative take-off height is the difference between the take-off height and the landing height. B: Take-off distance and landing distance as a function of the take-off angle. C: Take-off speed as a function of the take-off angle. D: Jump distance as a function of the take-off angle. E: Jump distance, flight distance, take-off distance and landing distance as a function of the take-off angle. It should be noted that that the first one is equal to the sum of the last three. All of them retrieved from *Wakai et al.*[19]